

## NUMERICAL INVESTIGATION OF PUNCHING SHEAR STRENGTH OF SLAB-COLUMN CONNECTIONS

SHEREEN MAHMOUD<sup>1</sup>, HAMED SALEM<sup>2</sup>

<sup>1</sup> Assistant lecturer, Institute of Aviation Engineering and Technology, Giza, Egypt, (E-mail: shreen.mahmoud@iaet.edu.eg).

<sup>2</sup> Professor, Department of Structural Engineering, Cairo University, Giza, Egypt, (E-mail: hhadhoud@eng.cu.edu.eg).

### ABSTRACT

Flat slab system is commonly used because of aesthetic appearance and flexibility of architecture. The punching shear is the major drawback of this structural system. The punching shear causes sudden failure lead to total collapse in the structure. In this paper 3D models that follow the method of applied element (AEM) to analyze the behavior of interior column-slab connections exposed to vertical displacement. The aim of this paper to show the importance of providing various types of punching shear reinforcement in the connection and improve the capacity of column-slab connection to prevent the local failure. The numerical study involved twenty six full-scale interior column- slab connections. This study is divided into two groups in addition to a control model where this model has no punching shear strengthening. The first group has thirteen models with additional punching strengthening such as closed stirrups around the column. The second group contains thirteen models with additional punching strengthening such as multi leg stirrups. The ultimate load is compared among several models. The simulated results display that shear strengthening improve both of strength.

**KEYWORDS:** Applied element method(AEM); Extreme loading of structure(ELS)

### 1.Introduction

Punching failure usually occurs in a brittle mode under influence of concentrated load above column support. This failure occurs without warning due to invisibly internal cracks causing catastrophic disaster. General classification for the failure can be shown either flexural or shear connected with the initial failure modes; yielding of reinforcement or crushing of concrete and extended internal diagonal cracking. Punching shear is considered to be the main factor that control the designing of reinforced concrete elements such as flat slabs, spread footing or raft footings.



Punching shear exists on the column connections of slabs because of the extraordinary concentration of stress. The failure mode of punching shear is a brittle failure which is not desirable in designing of reinforced concrete as it causes unexpected failure without warning. Shear reinforcement is the direct method that is used to resist punching shear to enhance its deformation capacity and shear resistance. The most common kinds of slab shear reinforcement are closed stirrups, bent bars, shear stud, fibers, multi- leg stirrups, and inverted drop panel. Punching failure is brittle failure mainly occurs due to vertical load and unbalanced moment. A 3D nonlinear analysis was used by 'Extreme Loading for Structures' software program [1], this based on Applied Element Method. The behavior of structure up to collapse will be simulated by using Applied Element Method simulation. Effect of various kinds of shear reinforcement methods were investigated. Both strength and ductility are enhanced via reinforcement for resisting punching shear [2]. A significant improvement on the performance was observed in the shear-reinforced slab. The deformation capacity is tripled and the strength is doubled. Shear reinforcement is the direct method that is used to resist punching shear to enhance its deformation capacity and shear resistance. **Stefan et.al** [3] studied the punching shear on experimental test and numerical analyses. Three main parts investigated deformation capacity and strength of slabs submitted to punching. The variables were the slab thickness, the column size, the shear reinforcement form and quantity. The authors deduced that the cracks passing through the shear strengthening could contribute to the slab rotation ensuring the shear crack theory. **Marzouk.et.al** [4] studied seventeen samples with different size of column, compressive strength, slab thickness, and ratio of tensile reinforcement. HSC samples could be distributed into two classifications which were shear punching and flexure-punching failure. Low flexural RFT of slabs resulted in flexural punching failure, while high RFT ratios slabs increased the stiffness of slab and decreased the deformation capacity. **Moe** [5] evaluated of (HSC) shear capacity as it related the shear capacity to square root of compressive strength concrete. **Hawkins et. al.** [6] studied four isolated joints subjected to dynamic loading. The variables were flexural reinforcement ratios and ratios of gravity shear  $V_g/V_c$ . cracks at face column, yielding load of tension and compression bars above column, and tensile bars located within distance equal  $(c+2h)$  from center of column. Lateral deformation of the joint away from cracks happened due to slip of tensile reinforcement. **Micael et.al** [7] investigated four samples to investigate punching behavior of HSC slabs experimentally.



The samples had reduced scale with different compressive strength and different longitudinal reinforcement subjected to monotonic loading at column intermediate. Three of samples were investigated using (HSC) and the last one was examined with (NSC). The (NSC) sample was considered as a reference sample. (HSC) increased the punching capacity to 43% comparing with (NSC). Increasing reinforcement ratio headed to a small increase of the punching capacity. (HSC) rupture more brittle when comparing it with (NSC). **Aurelio et. al.** [8] presented a model for showing punching performance for samples which had no transverse RFT reliant on shear crack theory. The slab rotation capacity and punching load can be proved by the proposed failure that headed to enhance the ductility. This failure mechanism coupled with load rotation resulting from slab nonlinear analysis in bending can indicate the punching load. The punching shear can perfectly be valued via different factors as ratio of span-depth of slab, the yield strength, the greatest aggregate size, concrete strength, column size, flexural and slab depth ratio. When comparing 87 results of test, it was detected that this technique provides high quality results with coefficient of variation ratio 8%. **AbdulQader et.al** [9] studied five samples with (3mx2mx0.25m) with constant flexural reinforcement. The first sample was a control and had no swimmer bar, while other samples were strengthened by swimmer bars of diameters 8, 10, 12, and 14 mm. The deformation capacity, strength, and ductility were enhanced by using swimmer bars. Using swimmer bars improves the capacity of punching 17% and improved the failure mode to ductile. Using swimmer bars of the pyramid cage decreased the slab thickness so reducing the construction cost and avoided using drop panels. The swimmer bar size enhanced the failure load and delayed widening of the shear crack. Figure (2-3) displays sample reinforced with swimmer bars. **Luca et.al** [10] analyzed seven slab samples with dimensions (3m x3mx0.25m). In addition, nine ½ scale slab sample (1.5mx1.5mx0.125m) was examined to know the behavior of bent bars. Bent bars acted as shear and flexural strengthening. The punching strength was boosted by using bent bars significantly. Bent bars became antiquated and exchanged owing difficulty of construction of other strengthening techniques. Bent bars noticeably improved the deformation capacity and the punching strength. Moreover, the flexural RFT might be reduced without affecting the punching capacity.

## 2. Experimental program

### 2.1 Set up for testing

Numerical analysis is carried out on full-scale interior column-slab joints. Fifty models are analyzed using Extreme Loading for Structure software (ELS) [1] that tracks the Applied Element Method, AEM. A parametric study is carried out to investigate different punching strengthening methods. One model is developed as a control model where no punching strengthening is used, while the other twenty six models include additional punching strengthening. The slab model dimension is 3.0 m x 3.0 m x 300 mm supported on a 300 mm x 300 mm square column. The inflection points of the slab are assumed hinged, while the loading is applied through the column. To insure uniform load on the column stub, a 300 mm x 300 mm steel plate was inserted above the column. A concrete compressive strength of 25 N/mm<sup>2</sup> was used for both slab and column. Two groups of models were studied according to method of strengthening. First group was used to study the strengthening with closed stirrups around column, second one was strengthened with multiple-leg stirrups. Column-slab connections are subjected to vertical point loading acting on the column stub. Loading is applied in the form of a controlled displacement at the center of the column through a steel plate squared shape with 60 mm thickness. The tensile stresses in the connection region are induced at the bottom fiber of the slab. The slab is simply supported on its four sides on steel plates with dimensions 3 mx50 mmx50 mm as shown in Figure (1). The plates are free to rotate out of plane and the interface between them and the slab is considered not to carry tensile stresses. The analysis of Extreme loading for structure program considers the structure own-weight, flooring load and live load.

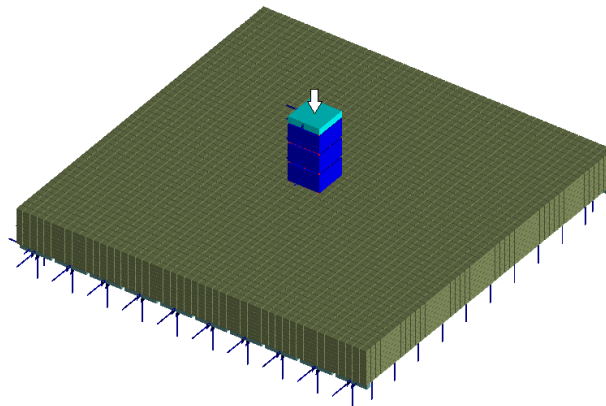


Figure1: Loading method on the developed three dimensional model using ELS.



## 2.2 Model Details and Mixture

For both slab and column, a concrete of compressive strength of  $25 \text{ N/mm}^2$  is used. Table 1 displays the concrete characteristics used for the model. For both slab and column, the tensile yield strength of reinforcement is  $360 \text{ N/mm}^2$ . Top reinforcement of ( $\Phi 10@160 \text{ mm}$  in every direction) and bottom reinforcement ( $\Phi 18@80 \text{ mm}$  in every direction) is used. Table 2 displays the reinforcement characteristics used for the model. The examined models are divided into two groups based on different kind of shear reinforcement to analyze performance of column- slab connections. In addition to the control specimen has no punching reinforcement. The control model is designed according to the Egyptian Code of Practice, ECP [11], The live and flooring loads are considered equal to  $2.5$  and  $2 \text{ kN/m}^2$ . The Egyptian Code of Practice (ECP) states the ultimate load combination of  $(1.4 D. L + 1.6 L. L)$ . The tension bottom reinforcement is  $\Phi 18/80 \text{ mm}$  in every direction and the compression top reinforcement is  $\Phi 10/160 \text{ mm}$  in every direction. There is no shear strengthening added in the control model. Figure 2 demonstrates plane and elevation of control model has no punching shear strengthening. Table 3 studied models strengthened by closed stirrups. Table 4 studied models strengthened by multiple leg stirrups.  $X_1$ : distance between the two branches of a stirrup (mm),  $X_2$ : distance between two successive stirrups (mm),  $X_3$ : distance covered by stirrups (mm),  $\Phi$ : diameter of stirrups (mm), and N: number of branches of stirrup.

**Table 1 characteristics of concrete**

Property	Value	Unit
Compressive Strength	25	$\text{N/mm}^2$
Tensile Strength	2.5	$\text{N/mm}^2$
Young's Modulus	2 E+5	$\text{N/mm}^2$
Shear Modulus	1 E+4	$\text{N/mm}^2$
Specific Weight	25	$\text{kN/m}^3$

**Table 2 characteristics of Reinforcing Steel**

Property	Value	Unit
Tensile Yield stress	360	N/mm <sup>2</sup>
Ultimate strength	520	N/mm <sup>2</sup>
Young's Modulus	2E+5	N/mm <sup>2</sup>
Shear Modulus	8E+4	N/mm <sup>2</sup>
Specific Weight	78.4	kN/m <sup>3</sup>

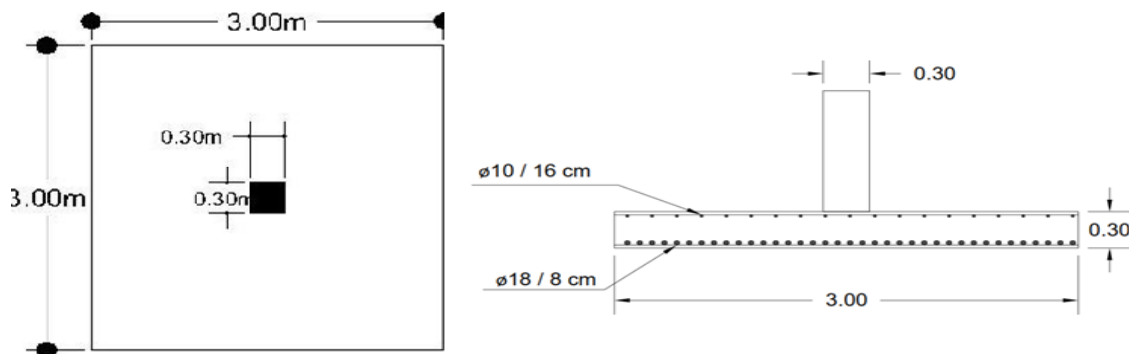


Figure 1 plan and Elevation of control model (no punching shear strengthening)



**Table 3 studied models strengthened by multiple leg stirrups**

Specimen	$X_1$ (mm)	$X_2$ (mm)	$X_3$ (mm)	$\Phi$ (mm)	N
C1 (Reference)	320	100	700	8	2
C2	480	100	700	8	2
C3	640	100	700	8	2
C4	320	150	700	8	2
C5	320	200	700	8	2
C6	320	100	700	12	2
C7	320	100	700	14	2
C8	320	100	700	16	2
C9	320	100	700	8	3
C10	320	100	700	8	4
C11	320	100	700	8	5
C12	320	100	500	8	2
C13	320	100	900	8	2

**Table 4 Studied models strengthened by Multiple leg stirrups**

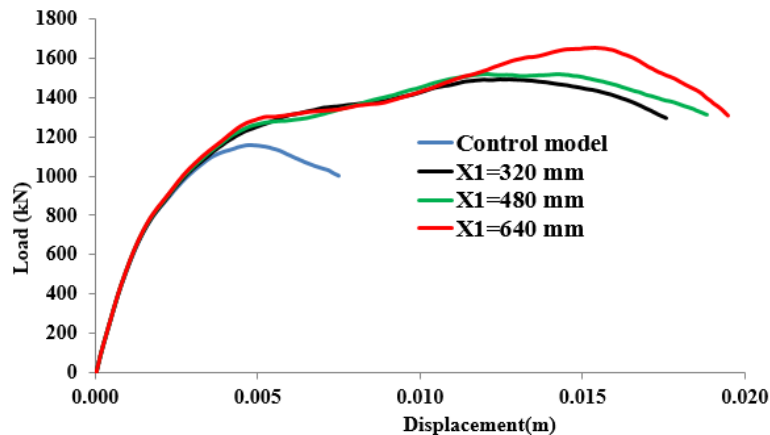
Model	X <sub>1</sub> (mm)	X <sub>2</sub> (m m)	X <sub>3</sub> (m m)	Φ (mm)	N
M1	320	100	800	8	2
M2	480	100	800	8	2
M 3	640	100	800	8	2
M4	320	150	800	8	2
M5	320	200	800	8	2
M6	320	100	800	12	2
M7	320	100	800	14	2
M8	320	100	800	16	2
M9	320	100	800	8	3
M10	320	100	800	8	4
M11	320	100	800	8	5
M12	320	100	500	8	2
M13	320	100	900	8	2

### 3. Discussions of numerical results

The numerical results discussed includes load-displacement curve for each model.

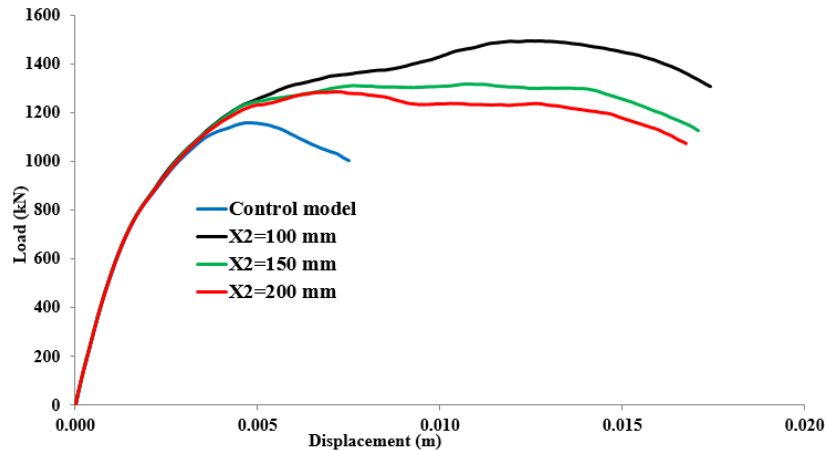
#### 3.1 Load -displacement curve for closed stirrups

Figure 3 displays the curve of load-displacement for models with various values of  $X_1$ . The model with  $X_1 = 640$  mm gives the highest ultimate load. The ultimate load increases with the increase of  $X_1$ . This may be explained that the larger the distance between the two branches of a stirrup, the more efficiency because of covering a great circumference of the inclined cracks. In other words, a better distribution of stirrups controlling the cracks more efficiently.



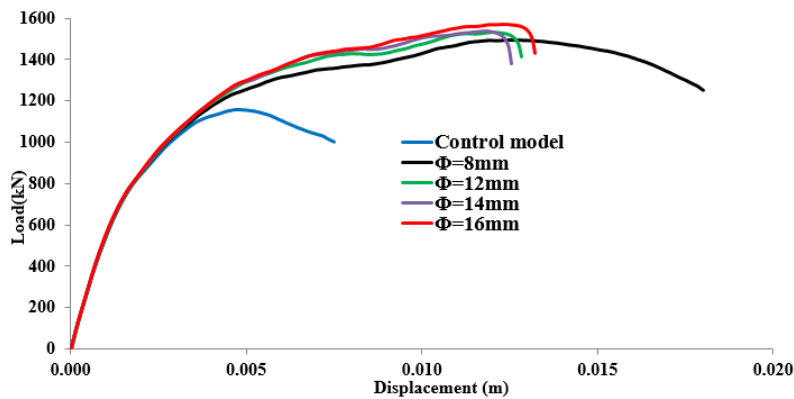
**Figure 3: Load-displacement curve for models with different  $X_1$**

Figure 4 shows the curve of load-displacement for each model with different values of  $X_2$ . The model with  $X_2 = 100$  mm gives the highest ultimate load. The ultimate load increases when the distance  $X_2$  decreases. This may be explained that the closer distance between two successive stirrups, the more their efficiency of closing the diagonal punching crack.



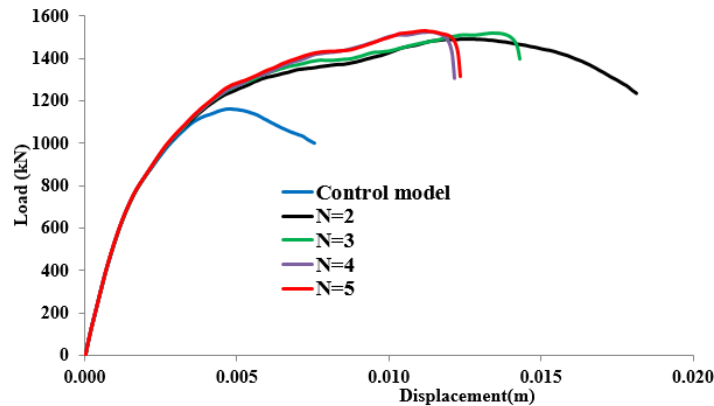
**Figure 4: Load-displacement curve for models with different distance  $X_2$**

. Figure 5 shows the curve of load-displacement for models with different values of  $\Phi$ . The model with  $\Phi=16$  mm gives the highest ultimate load. The ultimate load increases with the increase of  $\Phi$ . This may be explained that the bigger diameter of the stirrup, the more its efficiency because of preventing punching cracks at small load levels.



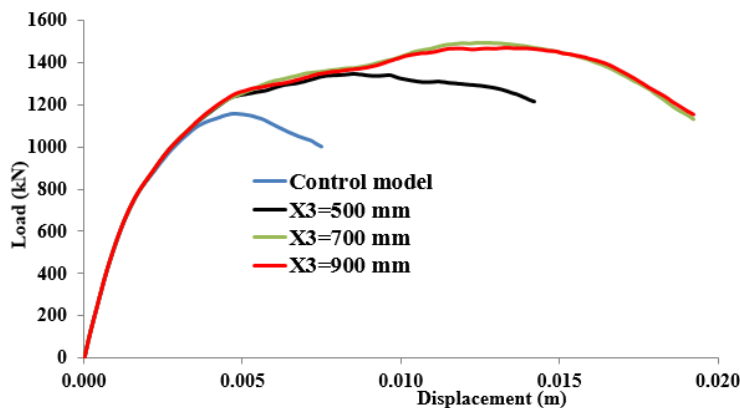
**Figure 5: Load-displacement curve for models of various  $\Phi$**

Figure 6 shows the curve of load-displacement for models with different values of N. The ultimate load slowly increases with the increase of N.



**Figure 6: Load-Displacement curve for models with different N**

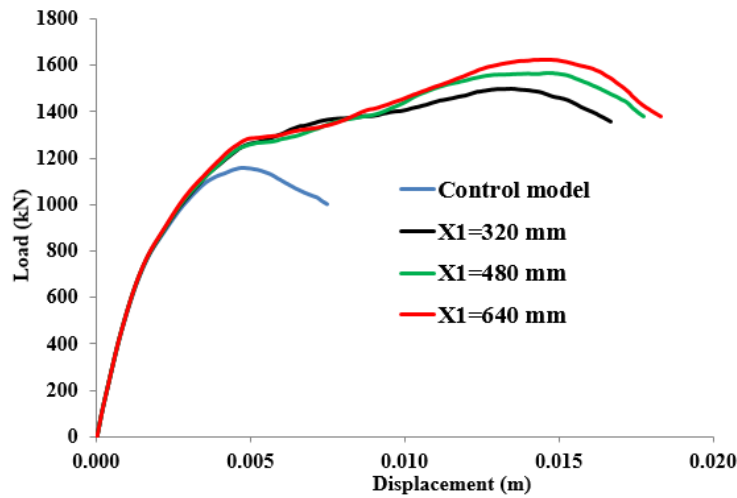
Figure 7 shows the curve of load-displacement for models with different values of  $X_3$ . Increasing  $X_3$  causes a slight increase in the model capacity. This is expected since increasing  $X_3$  results in covering large parts of diagonal cracks.



**Figure 7: Load-displacement curve for different distance  $X_3$**

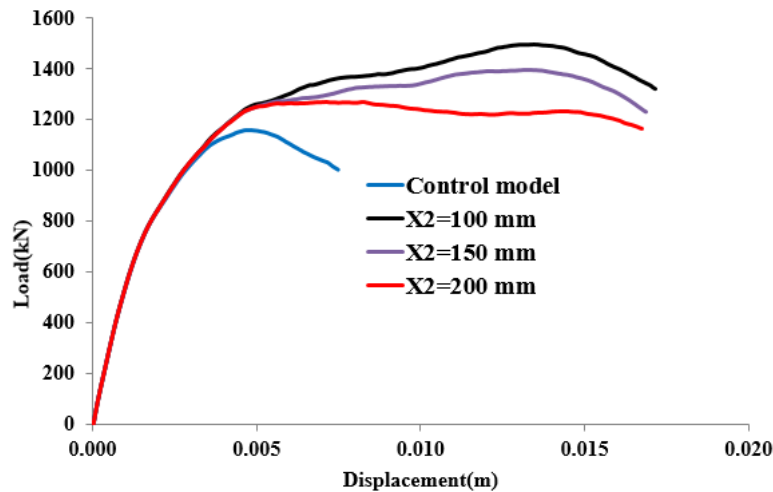
### 3.2 Load -displacement curve for multiple-leg stirrup

Figure 8 shows the curve of load-displacement for models with different values of  $X_1$ . The model with  $X_1=640$  mm gives the largest ultimate load. The ultimate load increases with the increase of  $X_1$ . This may be explained that the larger the distance between the two legs of a stirrup, the more efficiency because of covering a great circumference of inclined cracks. In other words, a better distribution of stirrups controlling the cracks more efficiently.



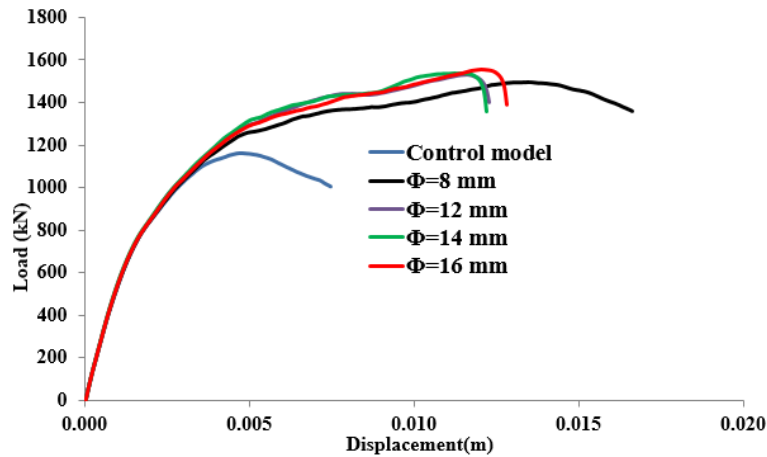
**Figure 8: Load-displacement curve for models with different  $X_1$**

Figure 9 shows the curve of load-displacement for modes with different values of  $X_2$ . The model with  $X_2=100$  mm clearly gives the greatest ultimate load, showing an increase in the capacity with smaller stirrups spacing's.



**Figure 8: Load-displacement curve for different distance  $X_2$**

. Figure 9 shows the curve of load-displacement for models with different values of  $\Phi$ . Increase of  $\Phi$  causes an increase in capacity. The model with  $\Phi=16$  mm gives the greatest ultimate load.



**Figure 9: Load-displacement curve for different diameters  $\Phi$**

. Figure 10 shows the load-displacement curve for models with different values of N. The increase of N causes an increase in capacity. The model with N=5 gives the greatest ultimate load.

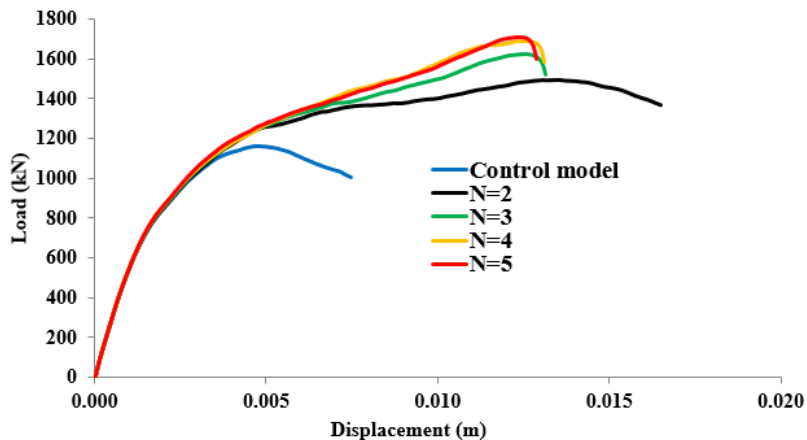


**Figure 10: Load-displacement curve for models with different N**

Figure 11 shows the curve of load-displacement for models with different values of  $X_3$ . Increasing  $X_3$  causes an increase in the model capacity. This is expected since increasing  $X_3$  result in covering large parts of diagonal cracks. The model with  $X_3=1000$  mm gives the greatest ultimate load.

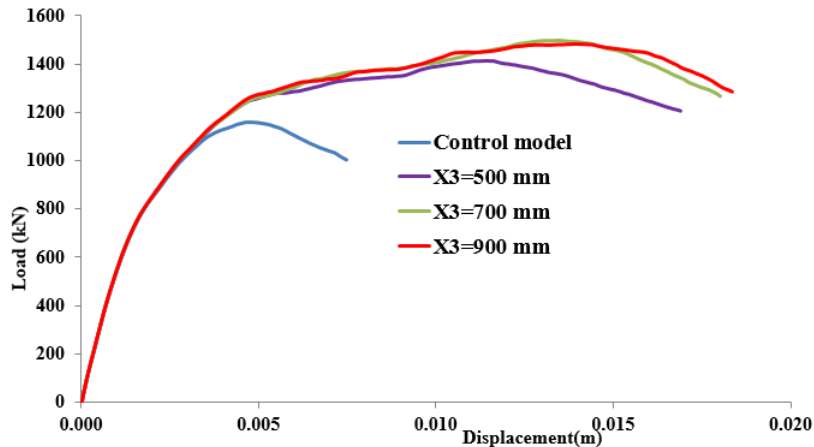


**Figure 11: Load-displacement curve for different distance  $X_3$**

## 4. Conclusion

The current research tends to numerically investigating the effects of various strengthening techniques to increase the punching strength of slab.

The numerical analyses are performed on interior joint of column-slab with a full scale. In addition, one is a control model without punching strengthening. The slab model dimensions are (3.00m $\times$ 3.00m $\times$ 0.30m) with a square column of (300mm  $\times$  300mm). Studied models are distributed to four groups according strengthening technique, namely, closed stirrups, multi leg stirrups, bent bars, and shear stud.

The numerical study was carried out using the Applied Element Method which was extensively validated in the literature and was partially validated for punching problems in the current study.

1. The ultimate punching capacity increases with the increase in distance between the two branches of a stirrup. A gain of 43% in capacity could be achieved for 640mm spacing. This gain is attributed to covering larger circumference of the diagonal cracks.



2. The ultimate punching capacity decrease with the increase in distance between two successive stirrups. A gain of 28% could be achieved for 100mm distance. This gain is attributed to covering larger area of the diagonal cracks.
3. The ultimate punching capacity increases with the increase in diameter of stirrups. A gain of 35% in capacity could be achieved for 16mm diameter. This gain is attributed to stirrups effect on preventing punching cracks.
4. The ultimate punching capacity increases with the increase of number of branches of stirrups. A gain of 32% in capacity be achieved for number of branches equal 5.
5. The ultimate punching capacity increase with the increase in distance covered by stirrups. A gain of 28.5% in capacity could be achieved for 900mm distance.
6. The ultimate punching capacity increase with the increase in distance between the two leg of a stirrup. A gain of 40% in capacity could be achieved for 640mm spacing.
7. The ultimate punching capacity decrease with the increase in distance between two successive stirrups. A gain of 29% in capacity could be achieved for 100mm distance.
8. The ultimate punching capacity increases with the increase in diameter of stirrup. A gain of 34% in capacity be achieved for 16mm diameter
9. The ultimate punching capacity increases with the increase in number of branches of stirrups. A gain of 47% in capacity be achieved for number of branches equal 5,
10. The ultimate punching capacity increase with the increase in distance cover by stirrups. A gain of 29% in capacity could be achieved for 1000mm distance. This gain is attributed to covering larger parts of diagonal crack.



## References

- [1] Stefan.LIPS, "Punching of Flat Slabs with Large Amounts of Shear Reinforcement," Suisse, 2012.
- [2] E. L. f. S. T. Manual, "http://www.extremeloading.com," ng for Structures Theoretical Manual, 2013. [Online].
- [3] Ramy Aly RoshdySadik, "INVESTIGATE WAYS TO ENHANCE DUCTILITY OF SLAB - COLUMN CONNECTIONS," Egypt, 2015.
- [4] R. H. E. Elstner, "Shearing Strength of Reinforced concrete slabs," Journal of the American Concrete Institute, vol. 28, no. 1, pp. 29-58, 1956.
- [5] J. Moe, "Shearing strength of reinforced concrete slabs and footings under concentrated loads," Portland Cement Association, Skokie, no. D47, p. 130, 1961.
- [6] a. H. A. Marzouk H., "Experimental investigation on the behavior of high- strength concrete slabs," ACI structural journal, vol. 88, no. 6, pp. 701-713, 1991.
- [7] N. M. D. a. S. M. S. Hawkins, "Cyclic behavior of six reinforced concrete slab-column specimens transferring moment and shear," Seattle, 1974.
- [8] A. R. V. L. a. D. F. Micael Inácio, "PUNCHING OF HIGH STRENGTH CONCRETE FLAT SLABS –EXPERIMENTAL INVESTIGATION," Portugal.
- [9] A. Muttoni, "Punching Shear Strength of Reinforced Concrete Slabs without Transverse Reinforcement," vol. 105, no. 4, pp. 440-450, August 2008.
- [10] A. S. Najmi, "Swimmer Bars as Shear Reinforcement in Reinforced Concrete Flat Slabs," vol. 4, no. 4, pp. 113-117, April 2015.
- [11] S. ., . Luca, "APPLICATIONS OF BENT-UP BARS AS SHEAR AND INTEGRITY REINFORCEMENT IN R/C SLABS," fib Symposium PRAGUE 2, Vols. Session 2B-5, pp. 631-634, 2011.
- [12] E. 203-07, "The Egyptian Code for Design and Construction of Concrete Structures," ministry of Housing, Cairo, Egypt, 2007.